



Effects of atmospheric CO₂ variability of the past 800 ka on the biomes of Southeast Africa

Lydie M. Dupont¹, Thibaut Caley², Isla S. Castañeda³

MARUM - Center for Marine Environmental Sciences, University of Bremen, Bremen, DE28359, Germany

² EPOC, UMR 5805, CNRS, University of Bordeaux, Pessac, Cs 50023, France

³ University of Massachusetts Amherst, Department of Geosciences, Amherst, MA 01003, USA

Correspondence to: Lydie M. Dupont (ldupont@marum.de)

Abstract. Very little is known about the impact of atmospheric carbon dioxide pressure ($p\text{CO}_2$) on the shaping of biomes. The development of $p\text{CO}_2$ throughout the Brunhes Chron may be considered a natural experiment to elucidate relationships between vegetation and $p\text{CO}_2$. While the glacial periods show low to very low values (~230 to ~190 ppmv, respectively), the $p\text{CO}_2$ levels of the interglacial periods vary from intermediate to relatively high (~250 to ~270, respectively). To study the influence of $p\text{CO}_2$ on the Pleistocene development of SE African vegetation, we used the pollen record of a marine core (MD96-2048) retrieved from Maputo Bay south of the Limpopo River mouth in combination with stable isotope and geochemical proxies. Applying endmember analysis, four pollen assemblages could be distinguished representing different biomes: heathland, mountain forest, shrubland and woodland. We find that the vegetation of the Limpopo River catchment and the coastal region of southern Mozambique is not only influenced by hydroclimate but by also temperature and atmospheric $p\text{CO}_2$. Our results suggest that the extension of either open ericaceous vegetation including C4 sedges or mountain forest depended on glacial $p\text{CO}_2$ levels, and that the main development of woodlands in the area took place after the Mid-Brunhes Event when interglacial $p\text{CO}_2$ levels rose over 270 ppmv.

20 1 Introduction

Understanding the role of atmospheric carbon dioxide pressure ($p\text{CO}_2$) is paramount for the interpretation of the of the paleo-vegetation record. The effects of low $p\text{CO}_2$ on glacial vegetation have been discussed in a number of studies [Ehleringer et al. 1997, Jolly & Haxeltine 1997, Cowling & Sykes 1999, Prentice & Harrison 2009, Prentice et al. 2017] predicting that glacial increase in C4 vegetation favoured by low atmospheric CO₂ would have opened the landscape and lowered the tree line. Comparing this open C4 rich vegetation with modern analogues would have led to an erroneous interpretation of the occurrence of arid adapted vegetation. These studies, however, mostly cover the Glacial Holocene transition and do not examine periods with intermediate $p\text{CO}_2$ such as during the early Glacial or interglacials prior to 430 thousand years ago (430 ka). Comparing the vegetation record of subsequent climate cycles showing different CO₂ levels might help to better understand the effects of $p\text{CO}_2$ on the vegetation.



During the Brunhes Chron (past 780 ka) the length of the glacial cycles became much longer lasting roughly 100 ka due to a strong non-linear response of the ice sheets to solar forcing [Mudelsee & Stategger 1997]. Model experiments of Ganopolski & Calov [2011] indicate that low atmospheric CO₂ concentrations are a prerequisite for the long duration of the glacial cycles of the past 800 ka. Then, roughly mid-way through the Brunhes Chron, the amplitude of the climate cycle shifted with a change

5 in the maximum CO₂ concentration during interglacials.

This so-called Mid-Brunhes Event (MBE) [Jansen et al. 1986] – also called Mid-Brunhes Transition – occurred about 430 ka ago and marks the transition between interglacials characterized by rather low atmospheric CO₂ around 240 ppm (parts of Marine Isotope Stages (MIS) 19, 17, 15, 13) to interglacials in which CO₂ levels reached 270 ppmv or more (parts of MIS 11, 9, 7, 5, 1) [Lüthi et al. 2008, Bereiter et al. 2015]. This climate transition has been extensively studied using Earth system

10 Models of Intermediate Complexity showing the necessity to include the change in atmospheric CO₂ in its explanation [Yin & Berger, 2010, 2012]. Additionally, Yin & Berger [2010] stress the importance of austral summer insolation, while Yin & Berger [2012] find that the modelled vegetation (tree-fraction) was forced by precession through precipitation at low latitudes. However, Yin [2013] concludes that it is not necessary to invoke an event around 430 ka to explain the increased interglacial

15 CO₂; the differences between interglacials can be explained by individual responses in Southern Ocean ventilation and deep-sea temperature to various combinations of the astronomical parameters. However, statistical analysis suggests a dominant role of the carbon cycle, which changed preceding the Mid-Brunhes Transition [Barth et al. 2018]. Paillard [2017] developed a conceptual model of orbital forcing of the carbon cycle in which sea-level fluctuations and the effects on carbon burial are decisive during shifts in the climate system. Further modelling by Bouttes et al. [2018] showed qualitative agreement with the paleodata of pre- and post-MBE interglacials but largely underestimated the amplitude of the changes. Moreover, the simulated

20 vegetation seems to counter the effects of the oceanic response [Bouttes et al. 2018]. Thus the vegetation, in particular at low latitudes, may play a crucial but poorly understood role in the climate system.

Comparing records of pre- and post-MBE interglacials could offer insight in the interglacial climate at different levels of CO₂ and the dynamical response of the vegetation, which has a positive feedback with temperature via land surface albedo and evapotranspiration [Foley et al. 1994, Swan et al. 2010]. We define interglacials after PAGES [2016] listing MIS 19c, 17c,

25 15a, 15e, 13a as pre-MBE and MIS 11c, 9e, 7e, 7a-c, 5e, 1 as post-MBE. Currently, only a handful of pollen records covering the entire Brunhes Chron have sufficient temporal resolution to enable comparisons between interglacials before and after the Mid-Brunhes transition. These records are from the eastern Mediterranean, arctic Siberia, the Colombian Andes [PAGES 2016] and East Africa [Castañeda et al. 2016, Johnson et al. 2016, Ivory et al. 2018, Owen et al. 2018]. The Andean pollen record is strongly influenced by the immigration of oak from North America during MIS 12 [Torres et al. 2013]. For the eastern

30 Mediterranean a decline in plant diversity is observed at Tenaghi Phillipon (Greece) with the gradual emergence of modern Mediterranean oak forests after MIS 16 but before the MBE [Tzedakis et al. 2006, 2009]. The El'gygytgyn vegetation record in eastern Siberia - resolved for MIS 31, 11c, 5e, and 1 - clearly indicates that the interglacials of MIS 31 (1081 - 1061 ka) and MIS 11c (422 - 394 ka) were warmer than those of MIS 5e (Last Interglacial) and MIS 1 (Holocene) [Melles et al. 2013]; Dark coniferous forest during MIS 11c was present instead of shrubland with birch and larch during MIS 5e and 1 forming the



climax vegetation in the high arctic [Lozhkin & Anderson 2013]. Additionally, stable carbon isotope records from Chinese loess sections indicate interglacial-glacial variability in the C3-C4 proportions of the vegetation [Lyu et al. 2018, Sun et al. 2019]. However, these records do not show a prominent vegetation shift over the MBE.

For East Africa two terrestrial records and a marine one are available. From Lake Malawi, Johnson et al. [2016] infer wetter conditions and increased woodland vegetation between 800 and 400 ka based on the stable carbon isotopic composition of plant wax shifting from less to more strongly depleted values. Also from Lake Malawi, Ivory et al. [2018] published a pollen record of the past 600 ka revealing a number of phases of miombo woodland and mountain forest alternating with savannah vegetation (dry woodland and wooded grassland). Recently, a new record from Lake Magadi (Kenya) has been published indicating a change from wetter conditions to more aridity after 500 ka contrasting the Lake Malawi results [Owen et al. 2018]. In Lake Magadi, the representation of *Podocarpus* decreased over the MBE, while open grassy vegetation and salinity of the lake increased [Owen et al. 2018]. Neither the Lake Malawi nor the Lake Magadi records show dominant interglacial-glacial variability.

The marine record retrieved south of the Limpopo River mouth (Core MD96-2048) allows inferences about vegetation and climate in the catchment area of the Limpopo River draining large areas of South Africa, Botswana, Zimbabwe and Mozambique. Based on sediment chemistry, Caley et al. [2018] reported the effects of increased summer insolation in increased fluvial discharge and variability associated with eccentricity, which modulates precession amplitudes. Superimposed on the orbital-scale precipitation variability, a long-term trend from 1000 to 600 ka towards increased aridity in south-eastern Africa was found [Caley et al. 2018]. The plant wax carbon isotopic record (hereafter $\delta^{13}\text{C}_{\text{wax}}$) of the same core was originally interpreted as reflecting a trend toward increasingly drier glacial and wetter interglacials over the past 800 ka [Castañeda et al. 2016]. The average and relative chain lengths of the plant leaf waxes exhibit a stepwise decrease at 430 ka suggesting a change from more shrub vegetation before the MBE to a larger contribution of trees during the post-MBE interglacials [Castañeda et al. 2016]. Thus, a pollen record of MD96-2048 has the potential to register the changes in interglacial vegetation cover over the MBE, which is expected to have had more pronounced effects on the Southern Hemisphere [Yin & Berger 2010]. However, the palynology of only the last 350 ka has been published [Dupont et al. 2011] and, therefore, here we extend the pollen record of MD96-2048 to cover the past 800 ka in sufficient resolution.

1.1 Previous work on Core MD96-2048

The sediments of MD96-2048 were retrieved in the middle of the Maputo Bight (Figure 1) from the southern Limpopo cone forming a depot centre that has been build up at least since the Late Miocene [Martin 1981]. The site collects terrestrial material including pollen and spores mostly from the rivers discharging into the Maputo Bight of which the Limpopo River is the biggest draining large areas of northern South Africa and southern Mozambique. Apart from the so-called Bergwinds, the predominant wind direction is landward [Tyson & Preston-Whyte 2000] and aeolian input of terrestrial material is probably minor. Thus, pollen source areas would cover the region north of the Maputo Bight in southern Mozambique and the region west of Maputo of the Lebombo hills and the Drakensberg Escarpment [Dupont et al. 2011].



A wide variety of measurements have been performed on MD96-2048 sediments. Caley et al. [2011, 2018] recorded stable oxygen isotopes of benthic foraminifers (*Planulina wuellerstorfi*) providing a stable oxygen stratigraphy and age model aligned to the global stack LR04 [Lisiecki & Raymo 2005] for the past 2200 ka. Trace element (Mg/Ca ratios) of the planktic foraminifer *Globigernoides ruber sensu stricto* and foraminifer assemblages were combined to produce a robust sea surface temperature (SST) record [Caley et al., 2018]. High resolution (0.5 cm) XRF-scanning has been performed over the total core length, of which the elemental iron over calcium ratios, $\ln(\text{Fe}/\text{Ca})$, were used to estimate fluvial terrestrial input variability [Caley et al., 2018]. At millennial resolution, higher plant leaf wax (*n*-alkane) concentrations and $\delta^{13}\text{C}_{\text{wax}}$ provided a record of vegetation changes in terms of open versus closed canopy and C4 versus C3 plants of the past 800 ka [Castañeda et al. 2016]. A very low resolution leaf wax deuterium isotopic record generated by Caley et al. [2018], in conjunction with other high-resolution proxies including $\ln(\text{Fe}/\text{Ca})$, was used to reconstruct rainfall and Limpopo River runoff during the past 2.0 Ma.

1.2 Present-day climate and vegetation

Modern climate is seasonal with the rainy season in summer (November to March). Yearly precipitation ranges from 600 mm in the lowlands to 1400 mm in the mountains, whereby rains are more frequent along the coast under the influence of SSTs [Jury et al. 1993, Reason & Mulenga 1999]. Annual average temperatures range from 24 to 16°C but in the highlands clear winter nights may be frosty.

The modern vegetation of this area belongs to the forest, Highveld grassland, and savannah biomes and also includes azonal vegetation (Figure 1) [Dupont et al. 2011 and references therein]. The natural potential vegetation of the coastal belt is forest, although at present it is almost gone; north of the Limpopo River mouth rain forests belong to the Inhambane phytogeographical mosaic and south of the Limpopo River the forest belongs to the Tongaland-Pondoland regional mosaic [White 1983]. The vegetation of the northern part of the Tongaland-Pondoland region is the Northern Coastal Forest [Mucina & Rutherford 2006]. Semi-deciduous forest is found in the Lebombo hills [Kersberg 1996]. Afromontane forest and Highveld grasslands grow along the escarpment and on the mountains. The savannahs of the Zambezi phytogeographical region including e.g. the miombo dry forest occur further inland [White 1983]. Azonal vegetation consists of freshwater swamps, alluvial, and seashore vegetation and mangroves [Mucina & Rutherford 2006].

2 Material and Methods

Pollen analysis of the 37.59 m long core MD96-2048 (26°10'S 34°01'E, 660m water depth) was extended with 65 samples down core to 12 m (790 ka). Average sampling distance for the Brunhes part was 7 cm reaching an average temporal resolution of 4 ka according to the age model based on the stable oxygen isotope stratigraphy of benthic foraminifers [Caley et al. 2011, 2018]. Two older windows have been sampled; 20 samples between 15 and 26 m (943-1537 ka) and 19 samples between 30 and 36 m (1785-2143 ka) were taken with an average resolution of 31 and 20 ka, respectively.



Pollen preparation has been described in [Dupont et al. 2011]. In summary, samples were decalcified with HCl (~10%), treated with HF (~40%) for two days, ultrasonically sieved over an 8- μ m screen and, if necessary, decanted. The samples were spiked with two *Lycopodium* spore tablets (either of batch #938934 or batch #177745). Residues were mounted in glycerol and pollen and spores examined at 400x or 1000x magnification. Percentages are expressed based on the total of pollen and spores ranging

5 from over 400 to 60 – only in six samples this sum amounts to less than 100. Confidence intervals (95%) were calculated after Maher [1972, 1981]. Pollen have been identified using the reference collection of African pollen grains of the Department of Palynology and Climate Dynamics of the University of Göttingen, the African Pollen Database collection, and literature [e.g. Bonnefille & Rioulet 1980, Scott 1982, Köhler & Brückner 1982, 1989, Schüler & Hemp 2016].

We assigned pollen taxa to groups such as riparian, woodland, forest, etc. (Supplementary Table 1) using information given

10 by Scott [1982], White [1983], Beentje [1994], Kersberg [1996], Coates-Palgrave [2002], Vincens et al. [2007]. Additionally, we carried out a multivariate analysis in the form of an endmember model unmixing procedure [Weltje, 1997], the statistics of which are specifically designed for the treatment of percentage data using a version of the unmixer algorithm programmed in MATLAB by Dave Heslop in 2008. Taxa occurring in 6 or more samples (listed in Supplementary Table 2) were used in the endmember modelling (148 of 231 taxa in 220 samples). We selected a model with four components explaining over 95%

15 of the variance ($r^2 = 0.953$). Iteration was stopped at 1000x resulting in a convexity at termination of -1.6881. Significance level at 99% for taxa to score on the assemblages was 0.018.

To study the correlations between different parameters, we used a linear regression model (least square regression) on linearly interpolated values (5 ka steps) from 0 to 790 ka. Correlation coefficients are given in Table 1. For interpolation and testing the correlation, we used the package PAST [Hammer et al. 2001].

20 **3 Result and Discussion**

3.1 Terrestrial input and provenance of the C4 plant wax

Pollen percentages of Cyperaceae (sedges) and Poaceae (grasses) are plotted in Figure 2 together with the $\delta^{13}\text{C}_{\text{wax}}$ of the *n*-alkane C_{31} and XRF-scanning data, $\ln(\text{Fe}/\text{Ca})$. Comparing the records of Cyperaceae and $\delta^{13}\text{C}_{\text{wax}}$ reveals that high relative amounts of C4 plant material co-varied with increased representation of sedges. They also co-varied with higher terrestrial

25 input indicated by $\ln(\text{Fe}/\text{Ca})$, and increased precipitation as suggested by deuterium of the C_{31} *n*-alkane [Caley et al., 2018]. We substantiated the correlations for the Brunhes Chron between pollen percentages, leaf waxes and elemental ratios in Table 1. Leaf wax data are after Castañeda et al. [2016] including Average Chain Length (ACL) of the C_{27} - C_{33} *n*-alkanes, the ratio of $\text{C}_{31}/(\text{C}_{31}+\text{C}_{29})$ and $\delta^{13}\text{C}_{\text{wax}}$ while $\ln(\text{Fe}/\text{Ca})$ ratios are from Caley et al. [2018]. Significant correlation is found between the leaf wax parameters and Cyperaceae data but not between $\delta^{13}\text{C}_{\text{wax}}$ (indicative of C4 inputs) and Poaceae pollen percentages,

30 although a correlation exists between Cyperaceae and Poaceae percentages. It is, therefore, likely that in sediments of MD96-2048 the C4 component of the plant wax originated mainly from C4 sedges. C4 sedges, of which papyrus is the most well-



known, are an important constituent of tropical swamps and riversides [Chapman et al. 2001]. Furthermore Cyperaceae pollen concentration (Figure 3) and percentages correlated with $\ln(\text{Fe}/\text{Ca})$ and the latter with $\delta^{13}\text{C}_{\text{wax}}$ (Table 1, Figure 2). The ratios of terrestrial iron over marine calcium can be interpreted as a measure for terrestrial input, which in this part of the ocean is mainly fluvial. Correlation between increased fluvial discharge and increased C4 vegetation as well as increased Cyperaceae pollen has been reported from sediments off the Zambezi [Schefuß et al. 2011, Dupont & Kuhlmann 2017]. Moreover, a fingerprint of C4 sedges was found in Lake Tanganyika [Ivory & Russel 2016]. As a consequence, material (leaf waxes and pollen) from the riverine vegetation is probably better presented than that from dry and upland vegetation. These results corroborate the reinterpretation of the $\delta^{13}\text{C}_{\text{wax}}$ record, in which the increased representation of C4 plants (*n*-alkanes enriched in ^{13}C) is instead attributed to stronger transport of material from the upper Limpopo catchment and the extension of swamps containing C4 sedges under more humid conditions [Caley et al., 2018]. Previously Castañeda et al. [2016] had interpreted increased C4 inputs as reflecting increased aridity.

Relatively low values of Cyperaceae pollen and Fe/Ca ratios are found for most interglacials of the Brunhes Chron (Figures 2 and 3), which could be interpreted as an effect of sea-level high-stands. However, Caley et al. [2018] demonstrated that the fluvial discharge is not related to sea-level changes. From the bathymetry of Maputo Bay, strong influence of sea-level is also not expected because the shelf is not broad and the locality of Core MD96-2048 is relatively remote on the Limpopo cone in the centre of the clockwise flowing Maputo Bight Lee Eddy. The eddy transports terrestrial material north-eastwards before it is taken southwards (Figure 1) [Martin 1981] and likely has not changed direction during glacial times. Thus, fluvial discharge was probably low during interglacials (among other periods), which might be the combined result of more evapotranspiration and less precipitation. It is remarkable that despite the drier conditions the representation of woodland and dry forest is relatively high during the interglacial periods (Figure 3, see also next section).

3.2 Endmembers representing vegetation on land

Palynological results have been published for the past 350 ka [Dupont et al. 2011] providing a detailed vegetation record for the past three climate cycles. Pollen and spore assemblages could be characterized by three so-called endmembers via endmember modelling (EM1, EM2, EM3). The assemblage of EM1 was dominated by *Podocarpus* (yellow wood) pollen percentages being more abundant during the non-interglacial parts of MIS 5, 7, and 9. EM2 was characterized by pollen percentages of Cyperaceae (sedges), Ericaceae (heath) and other plants of open vegetation and abundant during full glacial stages. EM3 constituted of pollen from woodland, forest, and coastal vegetation and was interpreted to represent a mix of several vegetation complexes.

We repeated the endmember modelling for the extended record covering the entire Brunhes Chron and the two early Pleistocene windows. With the extended dataset, cumulative increase of explanatory power lessened after four (instead of three) endmembers. Therefore, a model with four endmembers was chosen. We used the scores of the different pollen taxa on the endmember assemblages for our interpretation of the endmembers (list of taxa and scores in Supplementary Tables 1 and 2). We compare the new results with the previous analysis. Although the previous and current analysis show strong similarities,



we have given new names to the endmember assemblages reflecting our interpretation. A selection of pollen percentage curves are plotted together with each endmember fractional abundance in Supplementary Figures 1-4.

Of the now four endmember assemblages (Figure 3) one endmember has almost the same composition as EM2 [Dupont et al. 2011] of the previous analysis. Not only composition but also the fractional abundances, which were high during glacial stages, are very much alike. We name this endmember ‘E-Heathland’, which is dominated by Cyperaceae (sedges) pollen percentages followed by Ericaceae (heather) and hornwort (Anthocerotaceae) spores. Also *Lycopodium* (clubmoss) spore, Restionaceae and *Stoebe*-type pollen percentages score highest on this endmember. The E-Heathland assemblage represents a Fynbos-like open vegetation growing during full glacials. Other pollen records from SE Africa also indicate an open ericaceous vegetation with sedges and Restionaceae during glacial times [Scott 1999, Dupont & Kuhlmann 2017]. The record of MD96-2048 testifies that this type of open glacial vegetation regularly occurred since at least two million years.

Like the endmember EM1 [Dupont et al. 2011] of the previous analysis, one endmember is dominated by *Podocarpus* (yellow wood) pollen percentages. The assemblage is enriched by pollen of *Celtis* (hackberries) and *Olea* (olive trees) accompanied by undifferentiated fern spores. The interpretation as an assemblage representing mountain forest is rather straightforward and we name the assemblage ‘E-Mountain-Forest’. The fractional abundance of the E-Mountain-Forest is also high in glacials of the Brunhes Chron but not during the extremes. It is low in the early Pleistocene parts of the record.

The remaining endmember assemblages have no direct counterpart in the previous analysis, although summed together the pattern of fractional abundance is similar to that of EM3 [Dupont et al. 2011]. One endmember groups together 44 pollen taxa, mostly from coastal and dune vegetation, which we name ‘E-Shrubland’. It includes pollen of Asteraceae and Poaceae (grasses). The latter are not very specific as grass pollen values score almost as high on other endmember assemblages (E-Heathland and E-Shrubland). Several taxa scoring on this endmember are known from coastal or halophytic settings such as *Gazania*-type, Amaranthaceae, *Tribulus*, Acanthaceae and *Euphorbia*-type. Arboreal taxa in this assemblage are *Dombeya*, *Acacia*, Meliaceae/Sapotaceae. The most typical taxa are the *Buxus* species. We distinguished three types of *Buxus* pollen: *B. macowani*-type, *B. hildebrandtii* and *B. madagascariensis* [Köhler & Brückner 1982, 1989]. *B. madagascariensis* grows on Madagascar and the other two species inhabit bushland and forest on coastal dunes of the East African main-land. *B. hildebrandtii* nowadays is found in Somalia and Ethiopia and *B. macowani* is native in South Africa. The record of M96-2048 indicates that these *Buxus* species were more common in the early Pleistocene than during the Brunhes Chron.

The last endmember, which we name ‘E-Woodland’, groups together 39 pollen taxa from forest and woodland species with maximum values of less than 5 or 2% of the total of pollen and spores. To this assemblage belong *Pseudolachnostylis*, *Dodonaea viscosa* and *Manilkara*, which are woodland trees. *Protea* (sugarbush) and *Myrsine africana* (Cape myrtle) grow more upland and *Alchornea* is a pioneer forest tree often growing along rivers. Others include wide-range woodland taxa. The occurrence of pollen of *Brachystegia* (miombo tree), *Burkea africana*, *Spirostachys africana* and *Hymenocardia* in this assemblage is indicative of miombo dry forest and woodland. The assemblage additionally includes Rhizophoraceae pollen from the coastal mangrove forest. The fractional abundance of the E-Woodland assemblage is low during the early Pleistocene,



increased during the interglacials prior to the MBE and had maximum values during Interglacials 9e, 5e, and 1. These interglacials also exhibited maximum percentages of arboreal pollen excluding *Podocarpus*. In summary, the endmember analysis indicates a very stable open ericaceous vegetation with partially wet elements such as sedges and Restionaceae characterizing the landscape of full glacials. During the less extreme parts of the glacials, mountain *Podocarpus* forest was extensive as in most mountains of Africa [Dupont 2011, Ivory et al. 2018]. On the other hand, interglacials were characterized by coastal shrubs. In the course of the Brunhes Chron, the woody component, which was relatively weak before the MBE, became more and more important reflecting the same long-term trend found in the leaf wax records [Castañeda et al. 2016]. It is likely that the miombo dry forest and woodland developed in the region in the course of the Brunhes Chron. Particularly during Interglacials 9e and 1, the area might have been more forested than during the older interglacials of the Brunhes Chron.

3.3 Effects of atmospheric $p\text{CO}_2$

While the hydroclimate of the region shows precession variability [Caley et al. 2018], the vegetation is more affected by the glacial-interglacial pattern indicating that besides hydrology temperature and/or atmospheric $p\text{CO}_2$ levels were important drivers of the vegetation development. Combining the results of the pollen assemblages with stable carbon isotopes and element information indicates that during interglacials the region of SE Africa (northern South Africa, Zimbabwe, southern Mozambique) was less humid. The interglacial woodlands (represented by E-Woodland, Figure 4) would probably have grown under warmer and drier conditions than the glacial mountain forest (represented by E-Mountain-Forest). The increase in maximum $p\text{CO}_2$ levels during the post-MBE interglacials might have favoured tree growth.

The lack of trees during glacial extremes in the East and Southeast African Mountains might well be the result of low atmospheric $p\text{CO}_2$ in combination with low temperatures [Jolly & Haxeltine 1997]. Pollen records of mountain sites on both sides of the Congo basin showed some influence of CO_2 concentrations, which influence varied in the different environments [Izumi & Lézine 2016].

Moreover, the record of mountain forest in SE Africa indicates some extension of moist *Podocarpus* forest during those parts of the glacial stages with atmospheric $p\text{CO}_2$ exceeding ~ 220 ppmv (Figure 5). This holds also for the Interglacials 19c, 17c, 15e, 15a, 13a, and 7e, in which not only $p\text{CO}_2$ but also Antarctic temperatures were subdued. During Interglacials 11c, 9e, 7ac, 5e, and 1 the mountain forest is replaced by woodland (Figure 4). A picture emerges of cool glacial stages in SE Africa in which tree cover broke down when atmospheric $p\text{CO}_2$ became too low. It might be only after interglacial $p\text{CO}_2$ levels rose over ~ 250 ppmv that miombo woodland could establish in the area further extending during the warm and relatively dry post-MBE interglacials.

If interglacial climate was drier than most of the glacial in this part of the world, the question rises about the climatic implication of the ericaceous fynbos-like vegetation (represented by E-Heather, Figure 5) extending during full glacials over the mountains of South Africa – and correlating with the SST record. Singarayer & Burrough [2015] argued that the control of the Indian Ocean SSTs on the precipitation of South Africa shifted from a positive correlation during the interglacial to a negative



correlation during the Last Glacial Maximum. They invoked the effects of the exposure of the Sunda Shelf (Indonesia) on the Walker circulation causing a wetter region over the western Indian Ocean but also weaker easterly winds to transport moisture inland. To question the link between SST and precipitation in SE Africa even further, Caley et al. [2018] found that the precession signature in the river discharge proxy (Fe/Ca ratios) lacked in the SST record estimated on the same material. SE Africa could have been more humid during glacials if the temperature difference between land and sea increased.

5 Pollen records of ericaceous vegetation suggest an extensive open vegetation existing in the East African Mountains [e.g. Coetzee 1967, Bonnefille & Riollet 1988, Marchant et al. 1997, Debussche 1998, Bonnefille & Chalié 2000] and in SE Africa and Madagascar [e.g. Botha et al. 1992, Scott 1999, Gasse and Van Campo 2001, Scott & Tackeray 1987] during the last glacial. In our study, ericaceous fynbos-like vegetation (E-Heather) was found for those parts of the glacials having lower (less

10 than ~230 ppmv) atmospheric $p\text{CO}_2$ (Figure 5). Exceptions were found for MIS 12 and 14 when the difference of $p\text{CO}_2$ with that of the preceding stage was small [Barnola et al. 1987, Siegenthaler et al. 2005, Lüthi et al. 2008]. Dupont et al. [2011] argued that increase of C4 vegetation as the result of low $p\text{CO}_2$ was unlikely because no extension of grasses was recorded. However, this argument is flawed if sedges dominantly constituted the C4 vegetation in the area.

The increase in C4 vegetation during relative cool and humid climate would be in conflict with the idea that C4 plants are

15 more competitive in hot and dry climates [Ehleringer et al. 1997, Sage 2004]. However, this idea is mainly based on the ecology of grasses and the development of savannahs, while the C4 vegetation expansion in SE Africa during cool and humid phases is driven by sedges. A survey of the distribution of C4 sedges in South Africa revealed that those Cyperaceae do not have the same temperature constraints as C4 grass species [Stock et al. 2004]. More important, South African C4 sedges appear to have evolved under wetland conditions rather than under aridity. C4 *Cyperus* species even occur in the wettest parts of lower altitude

20 wetlands in KwaZulu-Natal [Kotze & O'Conner 2000]. Still, the C4/C3 sedge ratios in those wetlands decline with altitude and temperature. We presume, therefore, that the extension of C4 sedges during the more humid phases of the glacials is the result of low atmospheric CO_2 concentrations rather than of low temperatures.

3.4 Long-term trends in vegetation and climate of East Africa

The region of the Limpopo River becoming more and more wooded in the course of successive interglacials [Castañeda et al. 2016] somewhat paralleled the conditions around Lake Malawi [Johnson et al. 2016]. However, around Lake Malawi, forested phases of either mountain forest, seasonal forest, or miombo woodland alternating with savannahs occurred during both glacial and interglacial stages [Ivory et al. 2018]. Also in contrast to the Lake Malawi record, the MD96-2048 Poaceae pollen percentages fluctuated little and remained relatively low indicating that savannahs were of less importance in the Limpopo catchment area and the coastal region of southern Mozambique.

30 The trend to increased woodland in SE Africa after the MBE, noted at both Lake Malawi and in the Limpopo River catchment [Johnson et al. 2016, Caley et al. 2018, this study] contrasts with the development around the equator (and in the Northern Hemisphere). At the equator a trend to less forest around Lake Magadi marks the Mid-Brunhes transition [Owen et al. 2018]. Antiphase behaviour of SE African climate with that of West and East Africa emphasises the importance of the average position



of the tropical rainbelt shifting southwards during globally cold periods as has been inferred from Holocene to Last Glacial records of Lake Malawi [Johnson et al. 2002, Scholz et al. 2011]. Our results confirm that this relationship existed over the entire Brunhes Chron.

The Lake Malawi pollen record as well as that of the equatorial Lake Magadi in Kenya [Owen et al. 2018] do not show much of a glacial-interglacial rhythm and are dominated by the precession variability in tropical rainfall [cf. Clement et al. 2004]. Obviously, in the tropical climate of the Southern Hemisphere north of ~15°S the hydrological regime had more effect on the vegetation than changes in temperature, while further south the impact of temperature on the vegetation increased.

4 Conclusions

Palynology in combination with sediment chemistry and carbon isotope analysis of leaf waxes carried out on the marine sediments of MD96-2048 retrieved from the Limpopo River cone in Maputo Bay (SE Africa) allowed a detailed reconstruction of the vegetation developments over the Brunhes Chron and comparison with earlier Pleistocene vegetation of SE Africa.

Using endmember modelling, we could distinguish four pollen assemblages: E-Heathland, E-Mountain-Forest, E-Shrubland, and E-Woodland. The open sedge-ridge and ericaceous vegetation represented by E-Heathland occurred during those parts of the glacials with lower temperatures and atmospheric $p\text{CO}_2$. *Podocarpus*-rich mountain forest represented by E-Mountain-Forest extended during the less extreme parts of the glacials. E-Shrubland represents a shrub-like vegetation with coastal elements and *Buxus* species and mainly occurred during the earlier Pleistocene (before 1 Ma). E-Woodland represents interglacial woodlands, miombo woodland in particular, becoming more and more important in the successive interglacial stages of the Brunhes Chron and dominated the post-MBE interglacials.

Our results indicate strong influence of atmospheric $p\text{CO}_2$ fluctuations on the shaping of the biomes in SE Africa during the Brunhes Chron. During the colder phases of the glacials, low atmospheric $p\text{CO}_2$ might have favoured the extension of C4 sedges. Mountain forests could thrive during glacials as long as $p\text{CO}_2$ levels exceeded ~220 ppmv. Atmospheric $p\text{CO}_2$ levels over 250 ppmv might have been a prerequisite for the establishment of the miombo woodlands in SE Africa, which extended during the post MBE interglacials.

The vegetation record of the Limpopo catchment area showed more impact of glacial-interglacial variability and less effects of the hydroclimate compared to the more equatorial records of Lake Malawi and Lake Magadi. The long-term trend of increased woodiness in the course of the Brunhes Chron paralleled that of Lake Malawi but contrasted Lake Magadi suggesting a long-term southward shift in the average position of the tropical rainbelt.

References

Barnola, A., Raynaud, D., Korotkevich, Y.S., and Lorius, C.: Vostok ice core provides 160,000-year record of atmospheric CO_2 , *Nature*, 329, 408–414, doi:10.1038/329408a0, 1987.



- Barth, A.M., Clark, P.U., Bill, N.S., He, F., and Pisias, N.G.: Climate evolution across the Mid-Brunhes Transition, *Climate of the Past*, 14, 2071–2087, doi:10.5194/cp-14-2071-2018, 2018.
- Beentje, H.: Kenya trees, shrubs and lianas, National Museum of Kenya, Nairobi, 722p, 1994.
- Bereiter, B., Shackleton, S., Baggenstos, D., Kawamura, K., and Severinghaus, J.: Mean global ocean temperatures during the
5 last glacial transition, *Nature*, 553, 39–44, doi:10.1038/nature25152, 2018.
- Bonnefille, R. and Chalié, F.: Pollen-inferred precipitation time-series from equatorial mountains, Africa, the last 40 kyr BP, *Global and Planetary Change*, 26, 25–50, doi:10.1016/S0921-8181(00)00032-1, 2000.
- Bonnefille, R. and Riollet, G.: Pollens des savanes d'Afrique orientale, Éditions du Centre National de la Recherche Scientifique, Paris, 140p, 113pl, 1980.
- 10 Bonnefille, R. and Riollet, G.: The Kashiru pollen sequence (Burundi). Palaeoclimatic implications for the last 40,000 yr. B.P. in tropical Africa, *Quaternary Research*, 30, 19–35, doi:10.1016/0033-5894(88)90085-3, 1988.
- Botha, G.A., Scott, L., Vogel, J.C., and Von Brunn, V.: Palaeosols and palaeoenvironments during the Late Pleistocene Hypothermal in northern Natal, *South African Journal of Science*, 88, 508–512, 1992.
- Bouttes, N., Swingedouw, D., Roch, D.E., Sanchez-Goni, M.F., and Crosta, X.: Response of the carbon cycle in an intermediate
15 complexity model to the different climate configurations of the last nine interglacials, *Climate of the Past*, 14, 239–253, doi:10.5194/cp-14-239-2018, 2018.
- Caley, T., Extier, T., Collins, J.A., Schefuß, E., Dupont, L., Malaizé, B., Rossignol, L., Souron, A., McClymont, E.L., Jimenez-Espejo, F.J., García-Comas, C., Eynaud, F., Martinez, P., Roche, D.M., Jorry, S.J., Charlier, K., Wary, M., Gouvers, P.-Y., Billy, I., and Giraudeau, J.: A two-million-year-long hydroclimatic context for hominin evolution in southeastern Africa,
20 *Nature*, 560, 76–79, doi:10.1038/s41586-018-0309-6, 2018.
- Caley, T., Kim, J.-H., Malaizé, B., Giraudeau, J., Laepple, T., Caillon, N., Charlier, K., Rebaubier, H., Rossignol, L., Castañeda, I.S., Schouten, S., and Sinninge Damsté, J.S.: High-latitude obliquity as a dominant forcing in the Agulhas current system, *Climate of the Past*, 7, 1285–1296, doi:10.5194/cp-7-1285-2011, 2011.
- Castañeda, I.S., Caley, T., Dupont, L., Kim, J.-H., Malaizé, B., and Schouten, S.: Middle to Late Pleistocene vegetation and
25 climate change in subtropical southern East Africa, *Earth and Planetary Science Letters*, 450, 306–316, doi:10.1016/j.epsl.2016.06.049, 2016.
- Chapman, L.J., Balirwa, J., Bugenyi, F.W.B., Chapman, C., and Crisman, T.L.: Wetlands of East Africa: biodiversity, exploitation, and policy perspectives, Gopal, B, Junk, WJ & Davis, JA (Eds) *Biodiversity in Wetlands, Assessment, Funktion and Conservation*, Volume 2, Backhuys Publishers, Leiden, 101–131, 2001.
- 30 Clement, A.C., Hall, A., and Brocoli, A.J.: The importance of precessional signals in the tropical climate, *Climate Dynamics*, 22, 327–341, doi:10.1007/s00382-003-0375-8, 2004.
- Coates Palgrave, K.: *Trees of Southern Africa*, 3rd edition, revised and updated, Struik, Cape Town, 1212p, 2002.
- Coetzee, J.A.: Pollen analytical studies in east and southern Africa, *Palaeoecology of Africa*, 3, 146 p, 1967.



- Cowling, S.A. and Sykes, M.: Physiological significance of low atmospheric CO₂ for plant-climate interactions, *Quaternary Research*, 52, 237–242, doi:10.1006/qres.1999.2065, 1999.
- Debusk, G.H.: A 37,500-year pollen record from Lake Malawi and implications for the biogeography of afro-montane forests, *Journal of Biogeography*, 25, 479–500, doi:10.1046/j.1365-2699.1998.2530479.x, 1998.
- 5 Dupont, L.M.: Orbital scale vegetation change in Africa, *Quaternary Science Reviews*, 30, 3589–3602, doi:10.1016/j.quascirev.2011.09.019, 2011.
- Dupont, L.M. and Kuhlmann, H.: Glacial-interglacial vegetation change in the Zambezi catchment, *Quaternary Science Reviews*, 155, 127–135, doi:10.1016/j.quascirev.2016.11.019, 2017.
- Dupont, L.M., Caley, T., Kim, J.-H., Castañeda, I., Malaizé, B., and Giraudeau, J.: Glacial-interglacial vegetation dynamics in
10 south eastern Africa coupled to sea surface temperature variations in the Western Indian Ocean, *Climate of the Past*, 7, 1209–1224, doi:10.5194/cp-7-1209-2011, 2011.
- Ehleringer, J.R., Cerling, T.E., and Helliker, B.R.: C₄ photosynthesis, atmospheric CO₂, and climate, *Oecologia*, 112, 285–299, doi:10.1007/s004420050311, 1997.
- Foley, J., Kutzbach, J.E., Coe, M.T., and Levis, S.: Feedbacks between climate and boreal forests during the Holocene epoch,
15 *Nature*, 371, 52–54, doi:10.1038/371052a0, 1994.
- Ganopolski, A. and Calov, R.: The role of orbital forcing, carbon dioxide and regolith in 100 kyr glacial cycles, *Climate of the Past*, 7, 1415–1425, doi:10.5194/cp-7-1415-2011, 2011.
- Gasse, F. and Van Campo, E.: Late Quaternary environmental changes from a pollen and diatom record in the southern tropics (Lake Tritrivakely, Madagascar), *Palaeogeography, Palaeoclimatology, Palaeoecology*, 167, 287–308, doi:10.1016/S0031-
20 0182(00)00242-X, 2001.
- Hammer, Ø., Harper, D.A.T., and Ryan, P.D.: PAST: Paleontological Statistics Software Package for Education and Data Analysis, *Palaeontologia Electronica*, 4(1), 1–9, 2001.
- Ivory, S.J. and Russell, J.: Climate, herbivory, and fire controls on tropical African forest for the last 60 ka, *Quaternary Science Reviews*, 148, 101–114, doi:10.1016/j.quascirev.2016.07.015, 2016.
- 25 Ivory, S.J., Lézine, A.-M., Vincens, A., and Cohen, A.S.: Waxing and waning of forests: Late Quaternary biogeography of southeast Africa, *Global Change Biology*, 2018, 1–13, doi:10.1111/gcb.14150, 2018.
- Izumi, K. and Lézine, A.-M.: Pollen-based biome reconstructions over the past 18,000 years and atmospheric CO₂ impacts on vegetation in equatorial mountains of Africa, *Quaternary Science Reviews*, 152, 93–103, doi:10.1016/j.quascirev.2016.09.023, 2016.
- 30 Jansen, J.H.F., Kuijpers, A., and Troelstra, S.R.: A mid-Brunhes climatic event: long-term changes in global atmosphere and ocean circulation, *Science*, 232, 619–622, doi:10.1126/science.232.4750.619, 1986.
- Johnson, T.C., Brown, E.T., McManus, J., Barry, S., Barker, P., and Gasse, F.: A high-resolution paleoclimate record spanning the past 25,000 years in southern East Africa, *Science*, 296, 113–132, doi:10.1126/science.1070057, 2002.



- Johnson, T.C., Werne, J.P., Brown, E.T., Abbott, A., Berke, M., Steinman, B.A., Halbur, J., Conteras, S., Grosshuesch, S., Deino, A., Lyons, R.P., Scholz, C.A., Schouten, S., and Sinninghe Damsté, J.S.: A progressively wetter climate in southern East Africa over the past 1.3 million years, *Nature*, 537, 220–224, doi:10.1038/nature19065, 2016.
- Jolly, D., and Haxeltine, A.: Effect of low glacial atmospheric CO₂ on tropical African montane vegetation, *Science*, 276, 786–788, doi:10.1126/science.276.5313.786, 1997.
- Jury, M.R., Valentine, H.R., and Lutjeharms, J.R.: Influence of the Agulhas Current on summer rainfall along the southeast coast of South Africa, *Journal of Applied Meteorology*, 32, 1282–1287, doi:10.1175/1520-0450(1993)032<1282:IOTACO>2.0.CO;2, 1993.
- Kersberg, H.: Beiheft zu Afrika-Kartenwerk Serie S: Südafrika (Moçambique, Swaziland, Republik Südafrika), Bl 7: Vegetationsgeographie, Gebrüder Bornträger, Berlin, 182p, 1996.
- Köhler, E. and Brückner, P.: De Pollenmorphologie der afrikanischen *Buxus*- und *Notobuxus*-Arten (Buxaceae) und ihre systemstische Bedeutung, *Grana*, 21, 71–82, doi:10.1080/00173138209427683, 1982.
- Köhler, E. and Brückner, P.: The genus *Buxus* (Buxaceae): aspects of its differentiation in space and time, *Plant Systematics and Evolution*, 162, 267–283, doi:10.1007/978-3-7091-3972-1_14, 1989.
- Kotze, D., and O'Connor, T.G.: Vegetation variation within and among palustrine wetlands along an altitudinal gradient in KwaZulu-Natal, South Africa, *Plant Ecology*, 146, 77–96, doi:10.1023/A:1009812300843, 2000.
- Lisiecki, L.E., and Raymo, M.E.: A Pliocene-Pleistocene stack of 57 globally distributed benthic δ¹⁸O records, *Paleoceanography*, 20, PA1003, 1–17, doi:10.1029/2004PA001071, 2005.
- Lozhkin, A.V., and Anderson, P.M.: Vegetation responses to interglacial warming in the Arctic: examples from Lake El'Gygytgyn, Far East Russian Arctic, *Climate of the Past*, 9, 1211–1219, doi:10.5194/cp-9-1211-2013, 2013.
- Lüthi, D., Le Floch, M., Bereiter, B., Blunier, T., Barnola, J.-M., Siegenthaler, U., Raynaud, D., Jouzel, J., Fischer, H., Kawamura, K., and Stocker, T.F.: High-resolution carbon dioxide concentration record 650,000–800,000 years before present, *Nature*, 453, 379–382, doi:10.1038/nature06949, 2008.
- Lyu, A., Lu, H., Zeng, L., Zhang, H., Zhang, E., and Yi, S.: Vegetation variation of loess deposits in the southeastern Inner Mongolia, NE China over the past ~1.08 million years, *Journal of Asian Earth Sciences*, 155, 174–179, doi:10.1016/j.jseaes.2017.11.013, 2018.
- Maher, L.J. Jr.: Nomograms for computing 0.95 confidence limits of pollen data, *Review of Palaeobotany and Palynology*, 13, 85–93, doi:10.1016/0034-6667(72)90038-3, 1972.
- Maher, L.J. Jr.: Statistics for microfossil concentration measurements employing samples spiked with marker grains, *Review of Palaeobotany and Palynology*, 32, 153–191, doi:10.1016/0034-6667(81)90002-6, 1981.
- Marchant, R., Taylor, D., and Hamilton, A.: Late Pleistocene and Holocene history at Mubwindi Swamp, Southwest Uganda, *Quaternary Research*, 47, 316–328, doi:10.1006/qres.1997.1887, 1997.
- Martin, A.K.: The influence of the Agulhas Current on the physiographic development of the northernmost Natal Valley (S.W. Indian Ocean), *Marine Geology*, 39, 259–276, doi:10.1016/0025-3227(81)90075-X, 1981.



- Melles, M., Brigham-Grette, J., Minyuk, P.S., Nowaczyk, N.R., Wennrich, V., DeConto, R., Anderson, P., Andreev, A., Coletti, A., Cook, T.L., Haltia-Hovi, E., Kukkonen, M., Lozhkin, A.V., Rosén, P., Tarasov, P., Vogel, H., and Wagner, B.: 2.8 Million years of Arctic climate change from Lake El'Gygytgyn, NE Russia, *Science*, 337, 315–320, doi:10.1126/science.1222135, 2012.
- 5 Mucina, L. and Rutherford, M.C.: The vegetation of South Africa, Lesotho and Swaziland, *Strelitzia*, 19 South African National Biodiversity Institute, Pretoria, 807p, 2006.
- Mudelsee, M. and Statterger, K.: Exploring the structure of the mid-Pleistocene revolution with advanced methods of time-series analysis, *Geologische Rundschau*, 86, 499–511, doi:10.1007/s005310050157, 1997.
- Owen, R.B., Muiruri, V.M., Lowenstein, T.K., Renaut, R.W., Rabideaux, N., Luo, S., Deino, A.L., Sier, M.J., Dupont-Nivet, G., McNulty, E.P., Leet, K., Cohen, A., Campisano, C., Deocampo, D., Shen, C-C., Billingsley, A., and Mbuthia, A.: Progressive aridification in East Africa over the last half million years and implications for human evolution, *PNAS*, 115, 44, 11174–11179, doi:10.1073/pnas.1801357115, 2018.
- 10 Paillard, D.: The Plio-Pleistocene climatic evolution as a consequence of orbital forcing on the carbon cycle, *Climate of the Past*, 13, 1259–1267, doi:10.5194/cp-13-1259-2017, 2017.
- 15 Past Interglacials Working Group of PAGES: Interglacials of the last 800,000 years, *Review of Geophysics*, 54, 162–219, doi:10.1002/2015RG000482, 2016.
- Prentice, I.C., and Harrison, S.P.: Ecosystem effects of CO₂ concentration: evidence from past climates, *Climate of the Past*, 5, 297–307, doi:10.5194/cp-5-297-2009, 2009.
- Prentice, I.C., Cleator, S.F., Huang, Y.H., Harrison, S.P., and Roulstone, I.: Reconstructing ice-age palaeoclimates: Quantifying low-CO₂ effects on plants, *Global and Planetary Change*, 149, 166–176, doi:10.1016/j.gloplacha.2016.12.012, 2017.
- 20 Reason, C.J.C., and Mulenga, H.: Relationships between South African rainfall and SST anomalies in the Southwest Indian Ocean, *International Journal of Climatology*, 19, 1651–1673, doi:10.1002/(SICI)1097-0088(199912)19:15<1651::AID-JOC439>3.0.CO;2-U, 1999.
- 25 Schefuß, E., Kuhlmann, H., Mollenhauer, G., Prange, M., and Pätzold, J.: Forcing of wet phases in southeast Africa over the past 17,000 years, *Nature*, 480, 509–512, doi:10.1038/nature10685, 2011.
- Scholz, C.A., Cohen, A.S., and Johnson, T.C.: Southern hemisphere tropical climate over the past 145 ka: Results of the Lake Malawi Scientific Drilling Project, East Africa, *Palaeogeography, Palaeoclimatology, Palaeoecology*, 303, 1–2, doi:10.1016/j.palaeo.2011.01.001, 2011.
- 30 Schüller, L. and Hemp, A.: Atlas of pollen and spores and their parent taxa of Mt Kilimanjaro and tropical East Africa, *Quaternary International*, 425, 301–386, doi:10.1016/j.quaint.2016.07.038, 2016.
- Scott, L.: Late Quaternary fossil pollen grains from the Transvaal, South Africa, *Review of Palaeobotany and Palynology*, 36, 241–278, doi:10.1016/0034-6667(82)90022-7, 1982.



- Scott, L.: Vegetation history and climate in the Savanna biome South Africa since 190,000 ka: a comparison of pollen data from the Tswaing Crater (the Pretoria Saltpan) and Wonderkrater, *Quaternary International*, 57–58, 215–223, doi:10.1016/S1040-6182(98)00062-7, 1999.
- Scott, L. and Thackeray, J.F.: Multivariate analysis of late Pleistocene and Holocene pollen spectra from Wonderkrater, Transvaal, South Africa, *South African Journal of Science*, 83, 93–98, 1987.
- Siegenthaler, U., Stocker, T.F., Monnin, E., Lüthi, D., Schwander, J., Stauffer, B., Raynaud, D., Barnola, J.-M., Fischer, H., Masson-Delmotte, V., and Jouzel, J.: Stable carbon cycle–climate relationship during the late Pleistocene, *Science*, 310, 1313–1317, doi:10.1126/science.1120130, 2005.
- Stock, W.D., Chuba, D.K., and Verboom, G.A.: Distribution of South African C3 and C4 species of Cyperaceae in relation to climate and phylogeny, *Austral Ecology*, 29, 313–319, doi:10.1111/j.1442-9993.2004.01368.x, 2004.
- Sun, Y., An, Z., Clemens, S.C., Bloemendal, J., and Vandenberghe, J.: Seven million years of wind and precipitation variability on the Chinese Loess Plateau, *Earth and Planetary Science Letters*, 297, 525–535, doi:10.1016/j.epsl.2010.07.004, 2010.
- Swann, A.L., Fung, I.Y., Levis, S., Bonan, G.B., and Doney, S.C.: Changes in Arctic vegetation amplify high-latitude warming through the greenhouse effect, *PNAS*, 107, 1295–1300, doi:10.1073/pnas.0913846107, 2010.
- Torres, V., Hooghiemstra, H., Lourens, L., and Tzedakis, P.C.: Astronomical tuning of long pollen records reveals the dynamic history of montane biomes and lake levels in the tropical high Andes during the Quaternary, *Quaternary Science Reviews*, 63, 59–72, doi:10.1016/j.quascirev.2012.11.004, 2013.
- Tyson, P.D. and Preston-Whyte, R.A.: *The weather and climate of Southern Africa*, Oxford University Press, Cape Town, 396p, 2000.
- Tzedakis, P.C., Hooghiemstra, H., and Pälike, H.: The last 1.35 million years at Tenaghi Philippon: revised chronostratigraphy and long-term vegetation trends, *Quaternary Science Reviews*, 25, 3416–3430, doi:10.1016/j.quascirev.2006.09.002, 2006.
- Tzedakis, P.C., Raynaud, D., McManus, J.F., Berger, A., Brovkin, V., and Kiefer, T.: Interglacial diversity, *Nature Geoscience*, 2, 753–755, doi:10.1038/ngeo660, 2009.
- Vincens, A., Lézine, A.-M., Buchet, G., Lewden, D., Le Thomas, A., and Contributors: African pollen database inventory of tree and shrub pollen types, *Review of Palaeobotany and Palynology*, 145, 135–141, doi:10.1016/j.revpalbo.2006.09.004, 2007.
- Weltje, G.J.: End-member modeling of compositional data: numerical-statistical algorithms for solving the explicit mixing problem, *Mathematical Geology*, 29, 503–549, doi:10.1007/BF02775085, 1997.
- White, F.: *The vegetation of Africa*, Natural Resources Research, 20 UNESCO, 356p, 3maps, 1983.
- Yin, Q.Z.: Insolation-induced mid-Brunhes transition in Southern Ocean ventilation and deep-ocean temperature, *Nature*, 494, 222–225, doi:10.1038/nature11790, 2013.
- Yin, Q.Z. and Berger, A.: Insolation and CO₂ contribution to the interglacial climate before and after the Mid-Brunhes Event, *Nature Geoscience*, 3, 243–246, doi:10.1038/ngeo771, 2010.



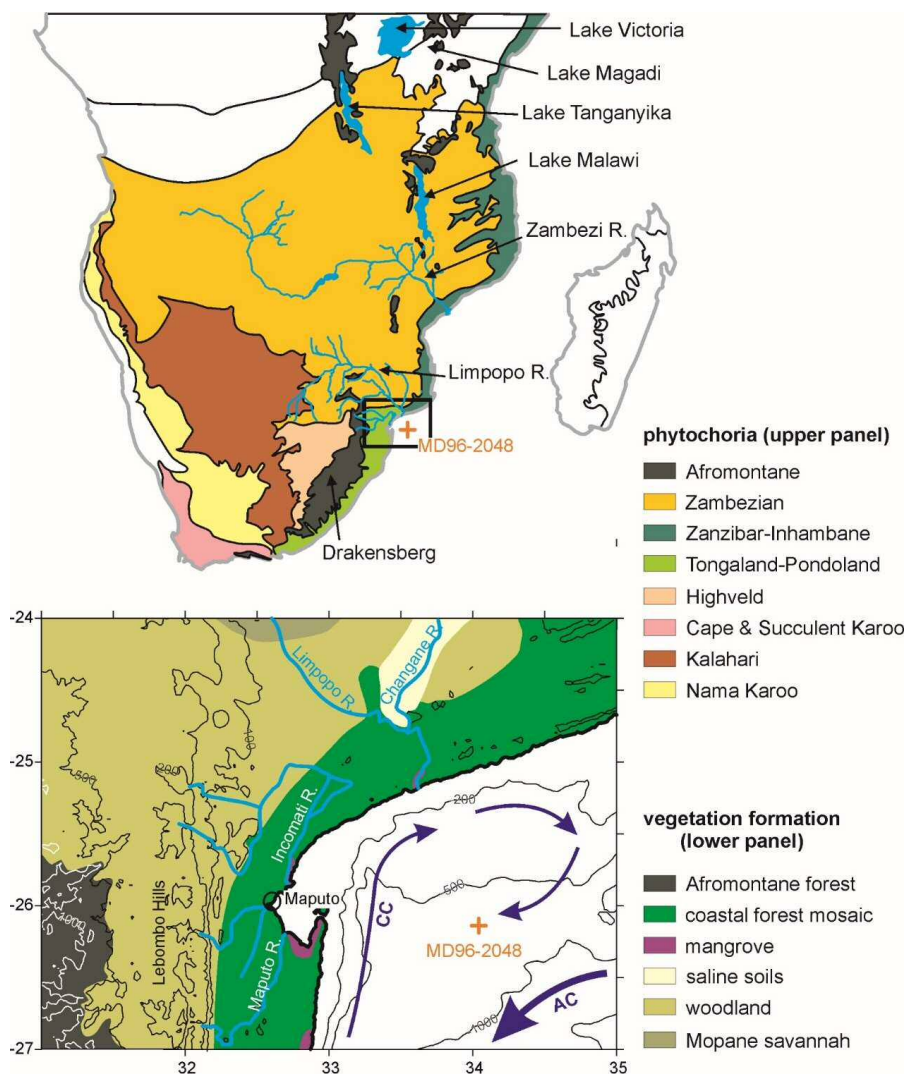
Yin, Q.Z. and Berger, A.: Individual contribution of insolation and CO₂ to the interglacial climates of the past 800,000 years, *Climate Dynamics*, 38, 709–724, doi:10.1007/s00382-011-1013-5, 2012.



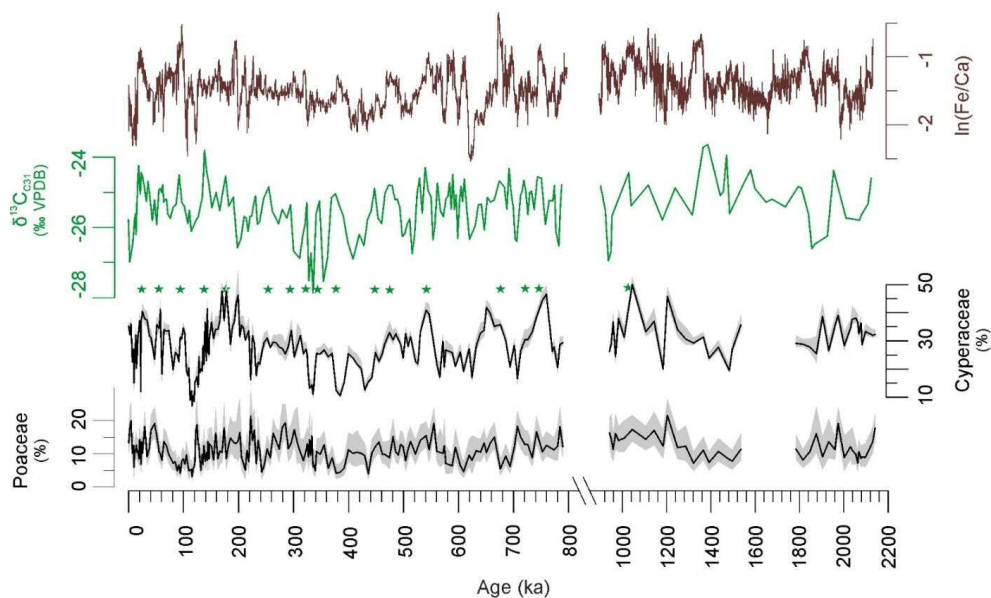
Table 1. Correlation coefficients calculated with PAST [Hammer et al 2001]. Significant correlations are underlined (95%) or bold and underlined (99%). Average Chain Length (ACL), ratio of concentrations of C₃₁/(C₃₁+C₂₉), and stable carbon isotope composition of the C₃₁ *n*-alkane ($\delta^{13}C_{wax}$) after Castañeda et al. [2016]. Cyperaceae and Poaceae pollen percentages (of total pollen and spores) after Dupont et al. [2011] and this study. XRF ln(Fe/Ca) data after Caley et al. [2018].

r ²	ACL	Ratio C ₃₁ /(C ₂₉ +C ₃₁)	$\delta^{13}C_{wax}$ (‰)	Cyperaceae (%)	Poaceae (%)	XRF ln (Fe/Ca)
ACL	1					
Ratio C ₃₁ /(C ₃₁ +C ₂₉)	<u>0.635</u>	1				
$\delta^{13}C_{wax}$	<u>0.079</u>	<u>0.180</u>	1			
Cyperaceae (%)	0.027	<u>0.140</u>	<u>0.142</u>	1		
Poaceae (%)	0.003	0.016	0.003	<u>0.165</u>	1	
XRF ln(Fe/Ca)	0.016	<u>0.032</u>	<u>0.227</u>	<u>0.110</u>	0.011	1

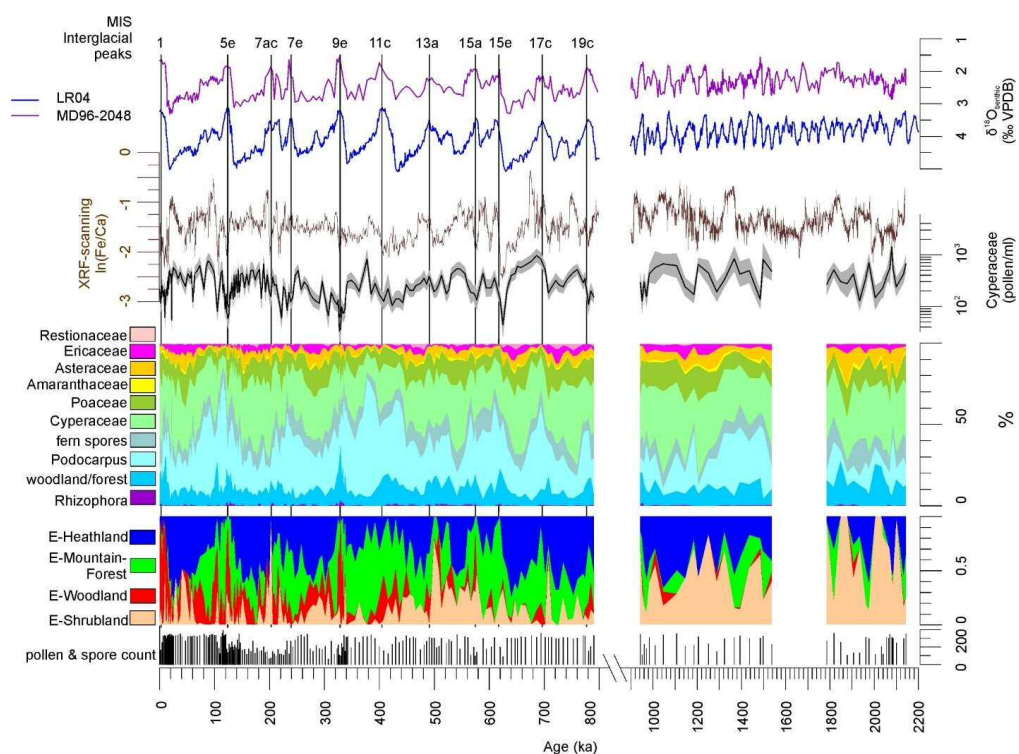
5



5 **Figure 1.** Upper panel: map of southern Africa with the main phytochoria after White (1983). Lower panel: site location of MD96-2048; main vegetation formations; main rivers; 100 m, 200 m, 500 m, and 1000m contours; 200 m, 500 m, and 1000m bathymetric contours; Agulhas (AC) and counter currents (CC) forming a coastal Maputo Bight Lee Eddy. Zambezian vegetation woodland and savannah north of $\sim 25^{\circ}30'S$, Tongaland-Pondoland coastal forests south of $\sim 25^{\circ}30'S$, Zanzibar-Inhambane coastal forests east of $33\text{--}34^{\circ}E$. West of the escarpment with Afromontane forest rises the interior plateau covered with Highveld grasslands.



5 **Figure 2.** Indicators of C4 vegetation and terrestrial input. From top to bottom: elemental Fe/Ca ratios [Caley et al. 2018], $\delta^{13}\text{C}_{\text{wax}}$ of the *n*-alkane C_{31} [Castañeda et al. 2016, Caley et al. 2018], Cyperaceae (sedges) pollen percentages, Poaceae (grass) pollen percentages. Shaded areas denote 95% confidence intervals after [Maher 1972]. Stars denote corresponding maxima in Cyperaceae pollen percentages and the stable carbon isotopes indicating C4 vegetation. VPDB: Vienna Pee Dee Belemnite.



5 **Figure 3. Summary of results of MD96-2048. Bottom to top: Pollen and spore count used to calculate percentages; Fractional abundance of endmembers E-Shrubland, E-Woodland, E-Mountain-Forest, E-Heathland; Pollen summary diagram (woodland and forest taxa are listed in Supplementary Table 1; Cyperaceae pollen concentration per ml (shading denote 95% confidence intervals after Maher [1981]; ln(Fe/Ca) after [Caley et al. 2018]; global stack of stable oxygen isotopes of benthic foraminifers, LR04 [Liesiecki & Raymo 2005]; $\delta^{18}\text{O}_{\text{benthic}}$ of Core MD96-2048 [Caley et al. 2018]; Interglacial peaks after PAGES [2016]. VPDB: Vienna Pee Dee Belemnite.**

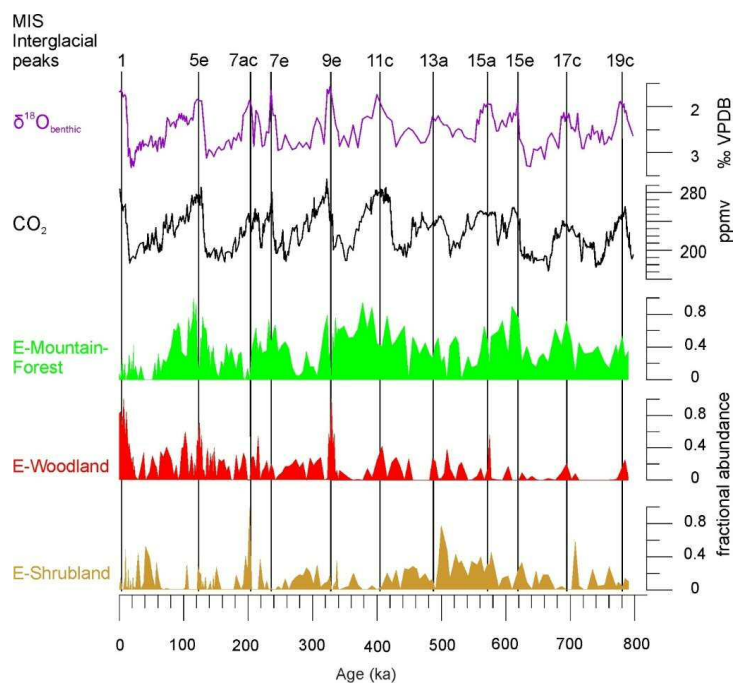


Figure 4: Comparing pollen assemblages E-Mountain-Forest, E-Woodland and E-Shrubland with atmospheric CO₂ [Barnola et al. 1987, Siegenthaler et al. 2005, Lüthi et al. 2008]. On top Interglacial peaks of the past 800 ka [PAGES 2016] and stable oxygen isotopes of benthic foraminifera ($\delta^{18}\text{O}_{\text{benthic}}$) of MD96-2048 [Caley et al. 2011]. VPDB: Vienna Pee Dee Belemnite.

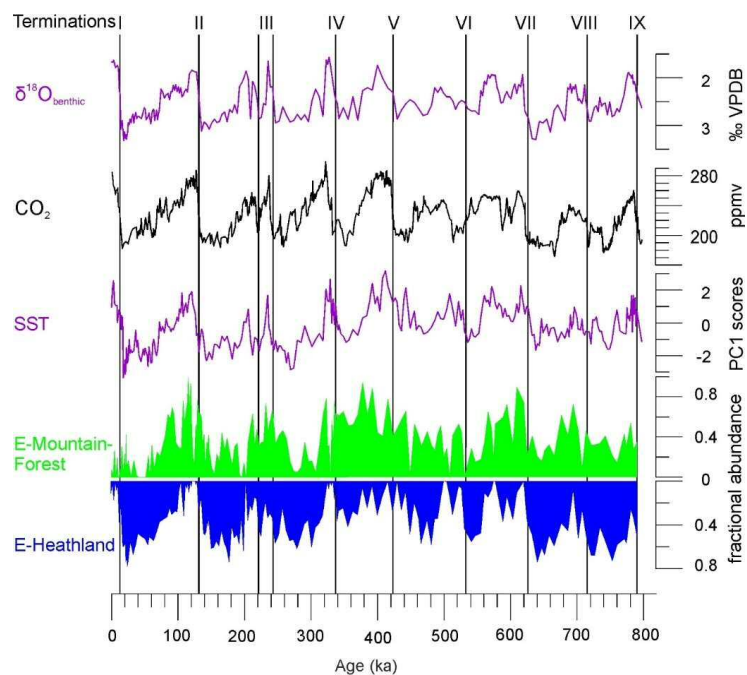


Figure 5: Comparing glacial pollen assemblages E-Mountain-Forest and E-Heather (reversed Y-axis) with atmospheric CO₂ [Barnola et al. 1987, Siegenthaler et al. 2005, Lüthi et al. 2008] and sea surface temperatures of the south-eastern Indian Ocean (SST PC1 scores of MD96-2048) [Caley et al. 2018]. On top Terminations of the past 9 glaciations and stable oxygen isotopes of benthic foraminifera ($\delta^{18}\text{O}_{\text{benthic}}$) of MD96-2048 [Caley et al. 2011]. VPDB: Vienna Pee Dee Belemnite.